

Co-design of a wave energy converter for autonomous power

Ryan G. Coe* Michael C. Devin*
Carlos A. Michelén Ströfer* Jantzen Lee* Giorgio Bacelli*
Alicia Keow* Daniel T. Gaebeler* Jeff Grasberger*
Steven J. Spencer* Johannes Spinneken** Vincent S. Neary*
Brek Meuris*

* Sandia National Laboratories, Albuquerque, NM 87123 USA
(e-mail: rcoe@sandia.gov)

** Evergreen Innovations, Sacramento, CA 95820 USA

Abstract: A “bolt-on” wave energy converter is designed to provide power for sensors on an existing oceanographic buoy. The narrow-banded pitch/roll response of the target oceanographic buoy lends itself to a tuned-resonator design, for which we suggest a novel “pitch resonator” wave energy converter concept. Using a pseudo-spectral method, the performance of the proposed wave energy converter is modeled in the range of sea states expected to be present at the target deployment location to study the effect of flywheel inertia on performance. The results show that the system can marginally meet the desired power demands, but suggest that related design concepts may be worth consideration.

Copyright © 2024 The Authors. This is an open access article under the CC BY-NC-ND license (<https://creativecommons.org/licenses/by-nc-nd/4.0/>)

Keywords: pseudo-spectral method; autonomous power; wave energy converter (WEC)

1. INTRODUCTION

Traditionally, wave energy converters (WECs) have been designed with the goal of maximizing large scale electricity generation in the service of meeting demand on electric grids. However, there is increasing interest in utilizing WECs in so-called “powering the blue economy (PBE)” applications, such as autonomous sensors, aquaculture systems, etc. (Hamilton et al., 2021; Cavagnaro et al., 2020; LiVecchi et al., 2019; Copping et al., 2018; Green et al., 2019). In PBE applications, the relevant power levels are generally lower along with the costs and risk levels. Additionally, the design requirements and drivers are distinct from grid-scale devices.

While a WEC delivering power to the grid must compete with other generation technologies capable of producing power with a levelized cost of energy (LCOE) on the order of \$0.05 per kWh, the PBE competition space looks quite different. It is not uncommon for oceanographic buoys to use non-rechargeable batteries, which must be replaced every few months. For a buoy located even 100 km offshore, the cost of replacing a battery may be considerable.

The levels of power that are relevant for PBE applications are quite small – often less than 20 W (Green et al., 2019). Counterintuitively, very small levels of consistent power can, in fact, represent a sizeable amount of energy for the long deployment periods relevant to oceanographic buoys. If an oceanographic buoy uses just 10 W of power for an entire year, that would amount to 88 kWh of total energy. For reference, a Tesla Powerwall 2 (0.12 m³, 114 kg, ~\$7.5k) can store 13.5 kWh of energy. Thus, while battery technology has certainly progressed rapidly in recent years, collocated power generation remains valuable.

This paper focuses on the design of a small WEC to power oceanographic sensors on the Coastal Surface Mooring (CSM) system within the National Science Foundation (NSF) funded Ocean Observatories Initiative (OOI) Pioneer Array. First, we introduce the concept for a “bolt-on” WEC which can be added to the existing CSM buoy. To support the detailed design of this device, we next present a numerical model to predict the WEC’s performance and apply this model to gain insight into a critical design aspect of the machine. The model presented here is well-suited to perform co-design studies on the WEC (note that the CSM design is considered “fixed”), as it can efficiently perform design sensitivity and optimization studies where the control and system design are considered in parallel.

2. BACKGROUND

2.1 Coastal Surface Mooring system

The Coastal Pioneer Array was originally located roughly 130 km south of Martha’s Vineyard, MA for its “New England Shelf” deployment. A second deployment at the Southern Mid-Atlantic Bight (MAB) between Cape Hatteras, NC and Norfolk Canyon (see Fig. 1) is currently proposed (Plueddemann et al., 2023), where the target mooring depth of at least one CSM within the array would be roughly 100 m. A detailed analysis of the site conditions for the proposed MAB deployment location were performed by Plueddemann et al. (2023). For our purposes in this study, we consider the seasonal wave conditions at this site (see Table 1). In particular, we will examine performance using the median wave conditions given the emphasis on consistent power generation from the WEC.

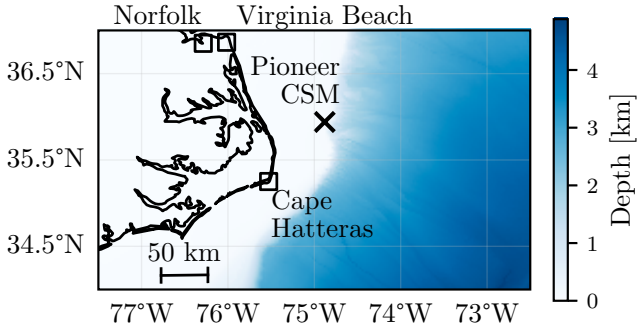


Fig. 1. Pioneer Array Coastal Surface Mooring proposed Mid-Atlantic Bight deployment location (bathymetry data source: GEBCO Compilation Group 2021).

Table 1. Median seasonal wave conditions (H_{m0} : significant wave height, T_e : energy period, T_p : energy period, J : energy flux, γ : peakedness factor) at Mid-Atlantic Bight.

	H_{m0} [m]	T_p [s]	T_e [s]	J [kW/m]	γ []
Winter	1.9	8.1	7.0	12.3	1.2
Spring	1.2	7.6	6.5	4.8	1.1
Summer	1.7	8.1	6.9	9.5	1.2
Fall	1.6	8.3	7.1	9.1	1.2

The CSM system (see Fig. 2) is an oceanographic mooring capable of taking measurements at the free surface, roughly 8 m below the free surface at the “Near Surface Instrument Frame (NSIF)”, and at the seabed (“Multi-Function node; MFN” in Fig. 2). The NSIF and MFN are connected via multiple sections of electromechanical (EM) stretch hose (Paul, 1995, 2004; Irish et al., 2005; Grosenbaugh et al., 2006), which allows the buoy to move relatively freely in waves and currents, preserving the validity of motion based measurements and reducing loading in extreme seas. Along with other assets within the Pioneer Array, the CSM is designed to take persistent measurements over multiple years to provide oceanographers, climate modelers, and other researchers with rich open-source datasets. Photos of the CSM are shown in Fig. 3.

The CSM is currently equipped with two Superwind SW350 wind turbines (rated 350 W each) and four 12 V Kyocera KD-140 photo-voltaic solar panels (rated 140 W each) which provide power to a battery bank. The typical system electrical load is 50-100 W depending on the specific sensor package, duty-cycling, and data telemetry rates. Due to various factors, including lulls in wind and solar resources as well as damage to the wind turbines and solar panels, the existing wind turbines and solar panels meet the full power demand of the CSM roughly 70% of the time, sometimes forcing the system to be manually throttled by shutting off lower priority operations. While the wind and solar resources will be somewhat different, based on an analysis of data collected during the New England Shelf deployment, it appears that an additional electrical generator capable of producing 10-20 W would be sufficient to give the CSM close to 100% up-time (Coe et al., 2023). Additionally, diversifying the electrical generation sources for the CSM is expected to generally produce a more robust system.

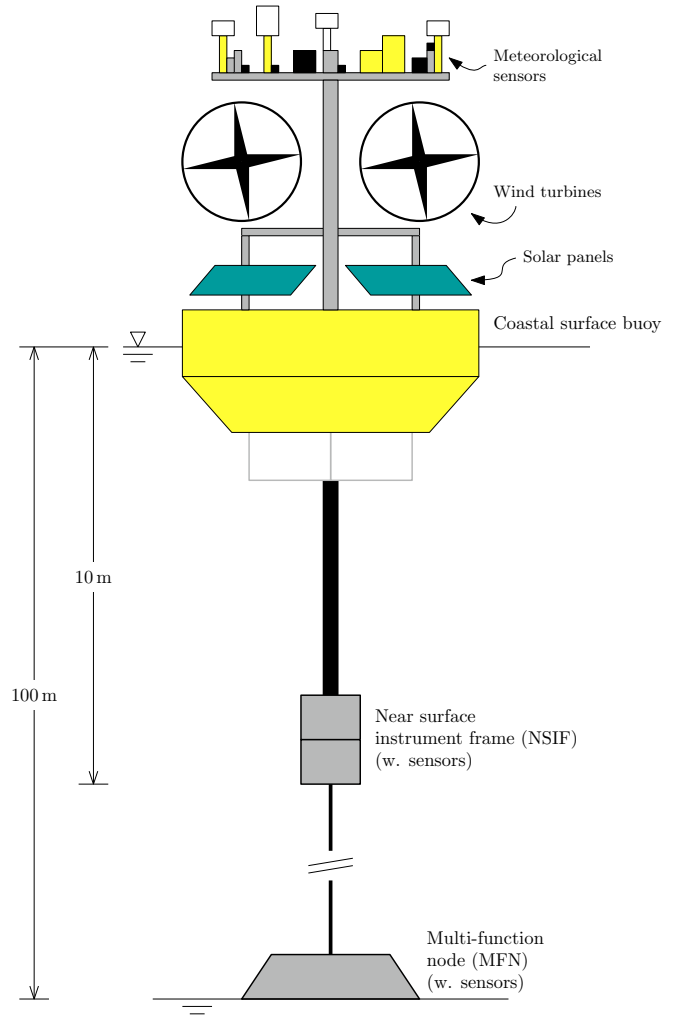
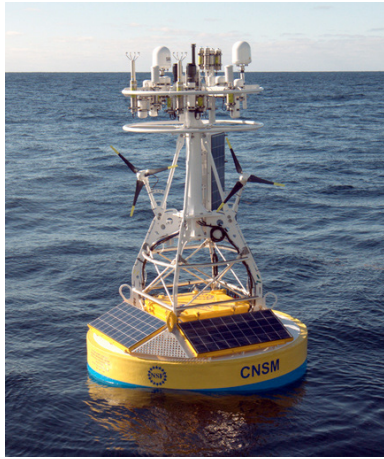


Fig. 2. Coastal Surface Mooring system diagram.

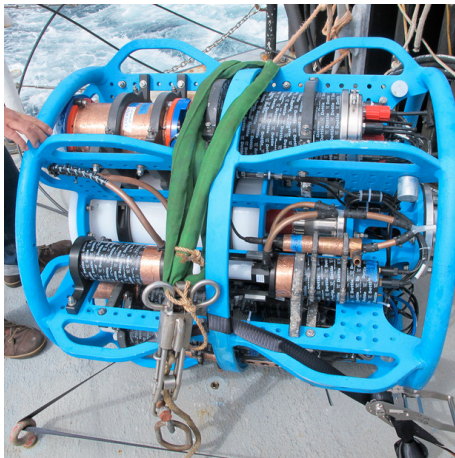
Analysis of data collected during the New England Shelf deployment shows that the pitch and roll responses of the CSM are very narrow-banded with a peak response of roughly 3 s (see Fig. 4). In deep water, a 3 s wave is approximately 14 m long – assuming a breaking steepness of 1/7, we should not expect waves of this period to exceed 2 m in height. In practice, this means that the pitch/roll motion of the buoy generally saturates at an amplitude of $\sim 15^\circ$ for even moderate sea states.

2.2 Pitch resonator concept

A number of design concepts were considered for WECs that could suit the needs of the CSM (Coe et al., 2023). Based on various considerations, the “pitch resonator” concept shown in Fig. 5 was selected. A flywheel with a moment of inertia J_{fw} , reacts against the buoy via a restoring stiffness (k_s) and electric motor/generator (τ_{pto}). Viscous and Coulumb friction between the buoy and flywheel are captured by b_f and μ_c , respectively. The subscripts ‘b’ and ‘fw’ relate to the buoy and flywheel, respectively. Note that Fig. 5 also illustrates the dynamics of the buoy’s pitch motion, where the buoy’s inertia J_b , the hydrostatic restoring effect is k_h , and the radiation damping effect is $B(\omega)$. The buoy is excited by a torque from the waves (τ_e), causing both the buoy and flywheel



(a) Surface buoy



(b) Near surface instrument frame (NSIF)



(c) Multi-function node (MFN)

Fig. 3. Pioneer Array Central Surface Mooring system components (source: Woods Hole Oceanographic Inst.).

to rotate – these absolute rotations are θ and ϕ in Fig. 5, respectively.

The linear dynamics system illustrated in the lower portion of Fig. 5 will be familiar to many readers from basic textbooks on dynamics (see, e.g., example problem A-5-2 in Ogata, 2004). The system is significantly more simple than similar moving mass WEC concepts that employ

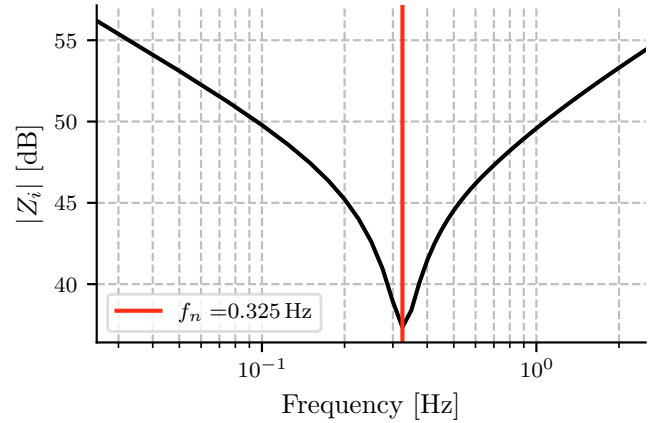


Fig. 4. Coastal Surface Mooring roll/pitch intrinsic impedance.

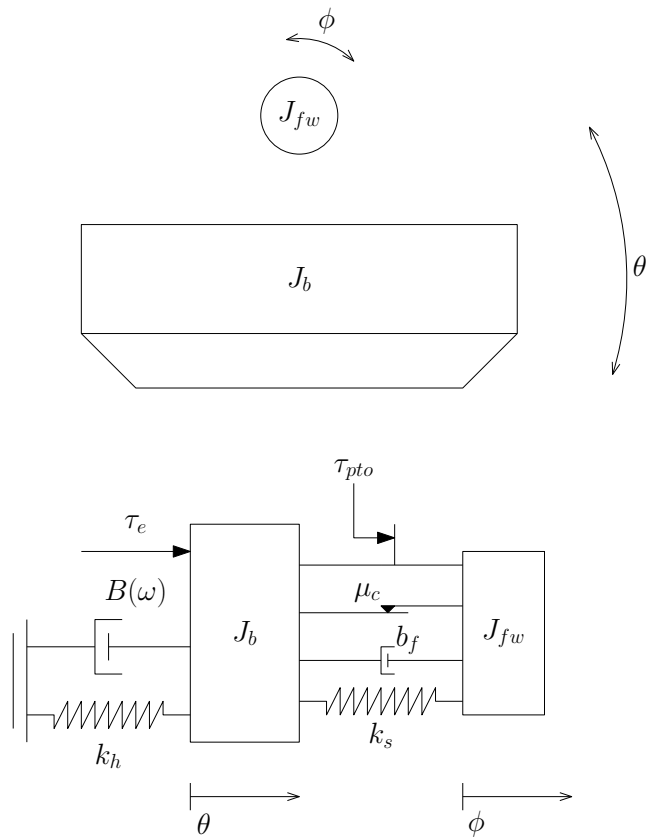


Fig. 5. Pitch resonator wave energy converter concept (upper: physical appearance; lower: equivalent dynamic system shown as linear motion system).

pendulums (Cordonnier et al., 2015; Nicola et al., 2017; Pasta et al., 2021; Gioia et al., 2022; Dizon and Brekken, 2022), because the center of gravity is located at the axis of rotation, thus avoiding chaotic behavior (Shinbrot et al., 1992; Dizon and Brekken, 2022).

The equations of motion for the pitch resonator system as illustrated in Fig. 5 can be expressed as

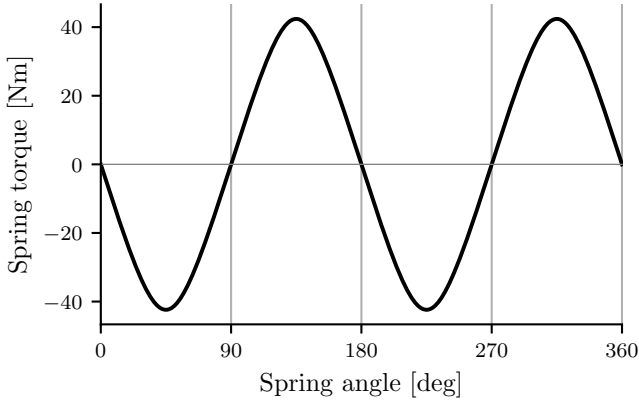


Fig. 6. Magnetic spring torque versus angular position.

$$(J_b + J(\omega))\ddot{\theta} = \tau_e - N_2\tau_{pto} - k_h\theta - B(\omega)\dot{\theta} - N_1^2k_s(\theta - \phi) - b_f(\dot{\theta} - \dot{\phi}) - \mu_c \quad (1a)$$

$$J_{fw}\ddot{\phi} = N_2\tau_{pto} + N_1^2k_s(\theta - \phi) + b_f(\dot{\theta} - \dot{\phi}) + \mu_c. \quad (1b)$$

The notation in (1) follows Fig. 5, with the addition of gears adjacent to the spring and motor (N_1 and N_2 , respectively). The electrical power from the motor/generator torque is captured with a 2-port impedance model (Michélen Ströfer et al., 2023).

$$\begin{bmatrix} \tau_{pto}(\omega) \\ V(\omega) \end{bmatrix} = \begin{bmatrix} -N_2^2Z_d(\omega) & -\sqrt{\frac{3}{2}}k_\tau N_2 \\ -\sqrt{\frac{3}{2}}k_\tau N_2 & Z_w(\omega) \end{bmatrix} \begin{bmatrix} U(\omega) \\ I(\omega) \end{bmatrix} \quad (2)$$

Here, $V(\omega)$ is the load voltage and $I(\omega)$ is the load current. The PTO velocity (the difference between $\dot{\theta}$ and $\dot{\phi}$) is $U(\omega)$. The motor torque constant is k_τ . The drivetrain and motor winding linear impedances are $Z_d(\omega)$ and $Z_w(\omega)$, respectively.

For the linear case where we give some closed-form expression for the PTO torque (e.g., a general impedance or some band-limited feedback control law), we may solve (1) analytically. However, given the applied nature of this project, we are interested in modeling the system dynamics with some additional nonlinearities, such as constraints on the PTO torque. Additionally, the spring envisioned for use in this system is a magnetic spring (Hossain et al., 2021; Che et al., 2021, 2022) with a periodic torsional response as shown in Fig. 6.

2.3 Pseudo-spectral model

A pseudo-spectral model for the pitch resonator WEC's performance was developed using `WecOptTool`¹. In this model, a solution for the optimal control trajectory can be obtained by defining a constrained optimization problem, in which the system dynamics are enforced as an equality constraint in residual form and the average electrical power is the objective function (Michélen Ströfer et al., 2023). Additional state and input constraints may be included if

¹ <https://sandialabs.github.io/WecOptTool>

Table 2. Key system parameters.

Parameter	Value
Flywheel moment of inertia, J_{fw} [kg m ²]	5..40
PTO spring, k_s [Nm/rad]	188..1880
PTO viscous friction, b_f [Nms/rad]	0.5
PTO Coulomb friction, b_c [Nm]	0.5
PTO spring gear ratio, N_1 []	0.333
PTO motor gear ratio, N_2 []	0.5
Motor torque const., k_τ [Nm/A]	3.512
Motor winding resistance [Ω]	0.304
Motor winding inductance [H]	0

desired. This analysis approach provides an ideal means of performing control co-design studies, in that the control algorithm and system design may be efficiently optimized together.

For the pitch resonator device examined in this study, we apply constraints on the maximum motor torque. Additionally, we include the nonlinear spring torque as illustrated in Fig. 6. The equations of motion from (1) are also extended to include this nonlinear spring torque and constrain the maximum motor torque to 120 Nm. Table 2 captures key parameters of the system as modeled herein.

3. RESULTS

For illustrative purposes, a time history for a regular wave with $H = 0.5$ m and $f = 0.325$ Hz (the resonant frequency of the system) is shown in Fig. 7. From Fig. 7, we can see that the PTO design is nearly achieving the biconjugate impedance matching condition (Bacelli and Coe, 2021) for this input frequency, but does still utilize some reactive power.

The flywheel moment of inertia is a high-level design variable. Heuristically, we expect that increasing the flywheel moment of inertia produce more power; however, given the desire to provide a “bolt-on” solution to the existing CSM system, limitations on space and buoyancy/stability will constrain the flywheel's size and weight. Here, we consider how the power produced varies for a range of flywheel inertias ($J_{fw} \leq 40$ kg m²) when properly matched with the appropriate spring stiffness to achieve the desired resonant frequency (f_n).

$$k_s = (2\pi f_n)^2 J_{fw} \quad (3)$$

Note that (3) disregards the fact that the spring is nonlinear (see Fig. 6). Given the nonlinear nature of the model at hand, we solve the pseudo-spectral problem for the irregular sea states using a frequency vector designed to sparingly capture the wave spectra and harmonics produced in the WEC response ($f = [0.075, 0.15, \dots, 2.25]$ Hz). A convergence study was employed to determine that 20 phase realizations could be used to robustly estimate average power for a given sea state.

The results of this analysis are shown in Fig. 8. As expected the higher inertia designs produce more power; more critically, we can see that, for the configuration modeled here, at flywheel moment of inertia on the order of 25 to 30 kg m² is needed to produce 10 W in the median wave conditions. Additionally, we can see that the median seasonal conditions in the winter months may produce

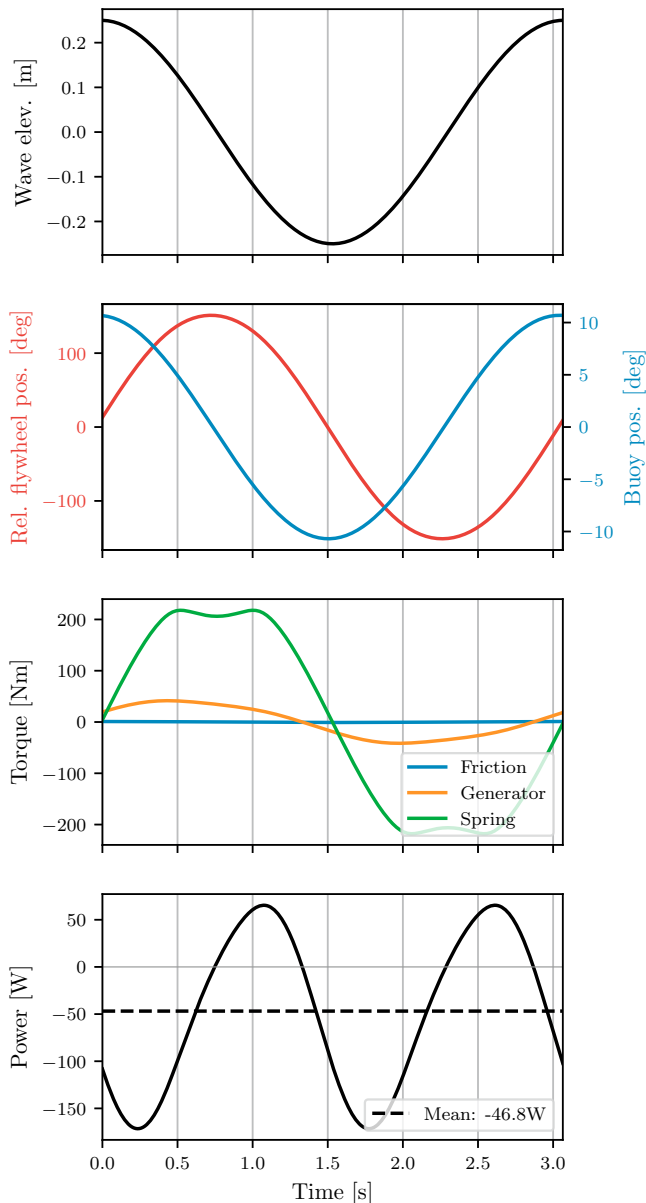


Fig. 7. Time history of buoy and pitch resonator response in a regular wave with $H = 0.5$ m and $f = 0.325$ Hz for a system with 25 kg m^2 flywheel.

roughly twice the power as the median conditions in the spring months.

4. DISCUSSION AND CONCLUSION

This paper examines the performance of a novel pitch resonator WEC concept on an existing oceanographic buoy in need of additional electrical power for scientific sensors. The expected performance is near the desired range and this model can be further applied to understand trade-offs between mass versus power, volume versus power, and related concepts. Comparing the results for irregular wave conditions (Fig. 8) with the sample results for a regular wave (Fig. 7), we also see that the pitch resonator performs much better in the regular wave simulation. Given the general nature of high quality factor tuned-mass-damper systems, this is somewhat expected, however

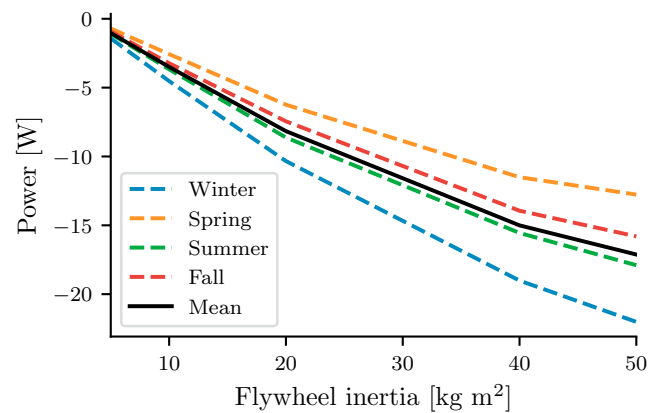


Fig. 8. Electrical power produced in median seasonal wave conditions at the Mid-Atlantic Bight deployment location using pitch resonator WECs with different levels of flywheel inertia.

the discrepancy here is quite strong. In this analysis, the numerical optimal control is utilized, so the results represent an upper bound for system performance. As such, related concepts with unbalanced flywheels are being considered and will be analyzed in future work. Additional work will assess the avoided cost of energy for this system based on field testing performance.

ACKNOWLEDGEMENTS

The work presented here builds on the broader Pioneer WEC project with contributions by Umesh Korde, Andrew Hamilton, Mike Muglia, Trip Taylor, Eric Wade, Al Plueddemann, John Reine, Don Peters, Derek Buffitt, Alex Franks, Sheri White, Kevin Dullea, Sahand Sabet, Salman Husain, and Scott Jenne. The authors would like to acknowledge funding support from the US Department of Energy's Water Power Technologies Office. Sandia National Laboratories is a multi-mission laboratory managed and operated by National Technology and Engineering Solutions of Sandia, LLC., a wholly owned subsidiary of Honeywell International, Inc., for the U.S. Department of Energy's National Nuclear Security Administration under contract DE-NA0003525. This paper describes objective technical results and analysis. Any subjective views or opinions that might be expressed in the paper do not necessarily represent the views of the U.S. Department of Energy or the United States Government.

REFERENCES

- Bacelli, G. and Coe, R.G. (2021). Comments on control of wave energy converters. *IEEE Transactions on Control Systems Technology*, 29(1), 478–481. doi: 10.1109/TCST.2020.2965916.
- Cavagnaro, R.J., Copping, A.E., Green, R., Greene, D., Jenne, S., Rose, D., and Overhus, D. (2020). Powering the blue economy: Progress exploring marine renewable energy integration with ocean observations. *Marine Technology Society Journal*, 54(6), 114–125. doi: 10.4031/MTSJ.54.6.11.
- Che, D., Bird, J.Z., Hagmüller, A., and Hossain, M.E. (2021). An adjustable stiffness torsional magnetic spring

- with a linear stroke length. In *2021 IEEE Energy Conversion Congress and Exposition (ECCE)*, 5944–5948. doi:10.1109/ECCE47101.2021.9595267.
- Che, D., Dechant, B., Hagmüller, A., and Bird, J.Z. (2022). A multi-stack variable stiffness magnetic torsion spring for a wave energy converter. In *2022 IEEE Energy Conversion Congress and Exposition (ECCE)*, 1–6. IEEE.
- Coe, R.G., Lee, J., Bacelli, G., Spencer, S.J., Dullea, K., Plueddemann, A.J., Buffitt, D., Reine, J., Peters, D., Spinneken, J., Hamilton, A., Sabet, S., Husain, S., Jenne, S., Korde, U., Muglia, M., Taylor, T., and Wade, E. (2023). Pioneer WEC concept design report. Technical Report SAND2023-10861, Sandia National Laboratories, Albuquerque, NM.
- Copping, A., LiVecchi, A., Spence, H., Gorton, A., Jenne, S., Preus, R., Gill, G., Robichaud, R., and Gore, S. (2018). Maritime renewable energy markets: power from the sea. *Marine Technology Society Journal*, 52(5), 99–109. doi:10.4031/MTSJ.52.5.3.
- Cordonnier, J., Gorintin, F., De Cagny, A., Clément, A., and Babarit, A. (2015). SEAREV: Case study of the development of a wave energy converter. *Renewable Energy*, 80, 40–52. doi:10.1016/j.renene.2015.01.061.
- Dizon, C. and Brekken, T. (2022). Relationship Between Power Output and Chaotic Behavior of a Pendulum PTO WEC. *IFAC-PapersOnLine*, 55(27), 132–137. doi:10.1016/j.ifacol.2022.10.500. 9th IFAC Symposium on Mechatronic Systems MECHATRONICS 2022.
- GEBCO Compilation Group (2021). GEBCO 2021 Grid. doi:10.5285/c6612cbe-50b3-0cff-e053-6c86abc09f8f.
- Gioia, D.G., Pasta, E., Brandimarte, P., and Mattiazzo, G. (2022). Data-driven control of a pendulum wave energy converter: A Gaussian process regression approach. *Ocean Engineering*, 253, 111191. doi:10.1016/j.oceaneng.2022.111191.
- Green, R., Copping, A., Cavagnaro, R.J., Rose, D., Overhus, D., and Jenne, D. (2019). Enabling power at sea: Opportunities for expanded ocean observations through marine renewable energy integration. In *OCEANS 2019 MTS/IEEE SEATTLE*, 1–7. doi:10.23919/OCEANS40490.2019.8962706.
- Grosenbaugh, M.A., Paul, W., Frye, D., and Farr, N. (2006). Development of synthetic fiber-reinforced electro-optical-mechanical cables for use with moored buoy observatories. *IEEE Journal of Oceanic Engineering*, 31(3), 574–584. doi:10.1109/JOE.2005.850937.
- Hamilton, A., Cazenave, F., Forbush, D., Coe, R.G., and Bacelli, G. (2021). The MBARI-WEC: a power source for ocean sensing. *Journal of Ocean Engineering and Marine Energy*, 7(2), 189–200. doi:10.1007/s40722-021-00197-9.
- Hossain, M.E., Bird, J.Z., Albarran, V., and Che, D. (2021). Analysis and experimental testing of a new type of variable stiffness magnetic spring with a linear stroke length. In *2021 IEEE Energy Conversion Congress and Exposition (ECCE)*, 5961–5965. doi:10.1109/ECCE47101.2021.9595241.
- Irish, J.D., Paul, W., and Wyman, D.M. (2005). The determination of the elastic modulus of rubber mooring tethers and their use in coastal moorings. Technical Report WHOI-2005-10, Woods Hole Oceanographic Institution, Woods Hole, Massachusetts.
- LiVecchi, A., Copping, A., Jenne, D., Gorton, A., Preus, R., Gill, G., Robichaud, R., Green, R., Geerlofs, S., Gore, S., et al. (2019). Powering the blue economy; exploring opportunities for marine renewable energy in maritime markets. Technical report, US Department of Energy, Office of Energy Efficiency and Renewable Energy. Washington, DC, Washington, DC.
- Michelén Ströfer, C.A., Gaebele, D.T., Coe, R.G., and Bacelli, G. (2023). Control co-design of power take-off systems for wave energy converters using WecOptTool. *IEEE Transactions on Sustainable Energy*, 14(4), 2157–2167. doi:10.1109/TSTE.2023.3272868.
- Nicola, P., Giovanni, B., Biagio, P., Antonello, S.S., Giacomo, V., Giuliana, M., and Gianmaria, S. (2017). Wave tank testing of a pendulum wave energy converter 1:12 scale model. *International Journal of Applied Mechanics*, 09(02), 1750024. doi:10.1142/S1758825117500247.
- Ogata, K. (2004). *System Dynamics*. Pearson/Prentice Hall, Upper Saddle River, NJ, 4 edition.
- Pasta, E., Carapellese, F., and Mattiazzo, G. (2021). Deep neural network trained to mimic nonlinear economic model predictive control: an application to a pendulum wave energy converter. In *2021 IEEE Conference on Control Technology and Applications (CCTA)*, 295–300. doi:10.1109/CCTA48906.2021.9659254.
- Paul, W. (1995). Design considerations for stretch conductors in oceanographic moorings. Technical Report WHOI-95-15, Woods Hole Oceanographic Institution, Woods Hole, Massachusetts.
- Paul, W. (2004). Hose elements for buoy moorings: Design, fabrication and mechanical properties. Technical Report WHOI-2004-06, Woods Hole Oceanographic Institution, Woods Hole, Massachusetts.
- Plueddemann, A., Macdonald, A., and Ramsey, A. (2023). CGSN Site Characterization: Pioneer Mid-Atlantic Bight Array. Technical Report 3210-00007, Woods Hole Oceanographic Institution.
- Shinbrot, T., Grebogi, C., Wisdom, J., and Yorke, J.A. (1992). Chaos in a double pendulum. *American Journal of Physics*, 60(6), 491–499. doi:10.1119/1.16860.